TISSUE ENGINEERING: Part A
Volume 25, Numbers 1 and 2, 2019

DOI: 10.1089/ten.tea.2017.0484

termis
Tissue Engineering
& Regenerative Medicine
International Society

SPECIAL FOCUS: RNA THERAPEUTICS FOR TISSUE ENGINEERING*

Acceleration of Diabetic Wound Healing with PHD2- and miR-210-Targeting Oligonucleotides

Anne Dallas, PhD,[1,**] Artem Trotsyuk, BS,[2,**] Heini Ilves, MS,[1,**] Clark A. Bonham, BS,[2] Melanie Rodrigues, PhD,[2] Karl Engel, BS,[2] Janos A. Barrera, MD,[2] Nina Kosaric, AB,[2] Zachary A. Stern-Buchbinder, MS,[2] Aleksandr White, MEng,[3] Kenneth J. Mandell, MD, PhD,[3] Paula T. Hammond, PhD,[4] Jonathan Mansbridge, PhD,[5] Sumedha Jayasena, PhD,[1,†] Geoffrey C. Gurtner, MD,[2] and Brian H. Johnston, PhD[1]

In diabetes-associated chronic wounds, the normal response to hypoxia is impaired and many cellular processes involved in wound healing are hindered. Central to the hypoxia response is hypoxia-inducible factor-1α (HIF-1α), which activates multiple factors that enhance wound healing by promoting cellular motility and proliferation, new vessel formation, and re-epithelialization. Prolyl hydroxylase domain-containing protein 2 (PHD2) regulates HIF-1α activity by targeting it for degradation under normoxia. HIF-1α also upregulates microRNA miR-210, which in turn regulates proteins involved in cell cycle control, DNA repair, and mitochondrial respiration in ways that are antagonistic to wound repair. We have identified a highly potent short synthetic hairpin RNA (sshRNA) that inhibits expression of PHD2 and an antisense oligonucleotide (antimiR) that inhibits miR-210. Both oligonucleotides were chemically modified for improved biostability and to mitigate potential immunostimulatory effects. Using the sshRNA to silence PHD2 transcripts stabilizes HIF-1α and, in combination with the antimiR targeting miR-210, increases proliferation and migration of keratinocytes *in vitro*. To assess activity and delivery in an impaired wound healing model in diabetic mice, PHD2-targeting sshRNAs and miR-210 antimiRs both alone and in combination were formulated for local delivery to wounds using layer-by-layer (LbL) technology. LbL nanofabrication was applied to incorporate sshRNA into a thin polymer coating on a Tegaderm mesh. This coating gradually degrades under physiological conditions, releasing sshRNA and antimiR for sustained cellular uptake. Formulated treatments were applied directly to splinted full-thickness excisional wounds in db/db mice. Cellular uptake was confirmed using fluorescent sshRNA. Wounds treated with a single application of PHD2 sshRNA or antimiR-210 closed 4 days faster than untreated wounds, and wounds treated with both oligonucleotides closed on average 4.75 days faster. Markers for neovascularization and cell proliferation (CD31 and Ki67, respectively) were increased in the wound area following treatment, and vascular endothelial growth factor (VEGF) was increased in sshRNA-treated wounds. Our results suggest that silencing of PHD2 and miR-210 either together or separately by localized delivery of sshRNAs and antimiRs is a promising approach for the treatment of chronic wounds, with the potential for rapid clinical translation.

Keywords: HIF-1α, miR-210, sshRNA, wound healing, PHD2, antimiR, diabetes

[1]SomaGenics, Inc., Santa Cruz, California.
[2]Department of Surgery, Stanford University School of Medicine, Stanford, California.
[3]LayerBio, Inc., Arlington, Massachusetts.
[4]Koch Institute, Massachusetts Institute of Technology, Cambridge, Massachusetts.
[5]Tecellact, Inc., La Jolla, California.
**All these authors contributed equally to this work.
[†]Current affiliation: NextMiRNA Technologies, Houston, Texas.

*This article is part of a special focus issue on RNA Therapeutics for Tissue Engineering.

Introduction

DIABETES AFFECTS ~25 million adults in the United States, with these numbers expected to double by the year 2050.[1] Approximately one-quarter of these patients develop at least one foot ulcer in their lifetime, increasing the risk of lower limb amputations.[2–4] The recurrence rate of diabetic ulcers is 66% and with subsequent ulcerations the amputation rate is 12%.[2] Nonhealing diabetic wounds are thus a tremendous challenge for patients and caregivers alike and cost the U.S. healthcare system $9–13 billion annually.[5,6] Microvascular impairments and dysfunctional neovascularization are the leading cause of pressure ulcers and chronic wounds in diabetic patients. These defects have been linked to a diminished cellular hypoxia response, of which the master regulator is the transcriptional factor, hypoxia-inducible factor-1α (HIF-1α).[7]

HIF-1α levels are negatively regulated by prolyl hydroxylase domain-containing protein 2 (PHD2), a crucial cellular oxygen sensor that hydroxylates two specific proline residues in HIF-1α, tagging it for rapid degradation via the proteasome pathway in normoxia.[8–11] However, in the hypoxic conditions of normal acute wounds, hydroxylation and degradation of HIF-1α are reduced, resulting in increased translocation of HIF-1α to the nucleus where it transactivates factors involved in vasculogenesis, angiogenesis, re-epithelialization, and cell survival that promote wound healing.[7–10] These include vascular endothelial growth factor (VEGF), erythropoietin (EPO), platelet-derived growth factor (PDGF), fibroblast growth factor (FGF), transforming growth factor beta (TGF-β), stromal cell-derived factor 1 (SDF-1), and heat shock protein 1 (HSP-1) (Fig. 1). In diabetic patients, induction of these factors is hampered due to high-glucose-induced modification of p300, a cofactor of HIF-1α transactivation.[12] Stabilization of HIF-1α may be achieved through inhibition of PHD2 expression,[8–10,13,14] and such intervention can improve wound closure in diabetic mice[8–10,13,14] (Fig. 1).

Hypoxia also induces the expression of certain microRNAs (miRNAs), called hypoxamirs, some of which are involved in wound healing.[15,16] One such miRNA, miR-210, is upregulated by HIF-1α[17–19] and targets E2F3, a cell cycle regulator that facilitates the G1/S transition. This activity is thought to be responsible for the finding that miR-210 attenuates keratinocyte proliferation as well as re-epithelialization in ischemic wound healing.[15] The stabilization of HIF-1α through pharmacological inhibition of PHD2 alone would be expected to upregulate miR-210, and have negative consequences for wound healing.

We therefore hypothesize that stabilization of HIF-1α via PHD2 inhibition might be most effective if miR-210 is also inhibited. Because of the ease of combining oligonucleotides in a delivery cocktail, we decided to use an RNA-based approach to accelerate the wound healing process by inhibiting each of these hypoxia response targets (Fig. 1). To inhibit expression of PHD2, we used a novel class of short synthetic hairpin RNAs (sshRNAs); such RNAs have previously been shown to be highly potent inhibitors of hepatitis C virus in mouse models.[20,21] sshRNAs induce cleavage of target RNAs by a novel Dicer-independent RNA interference (RNAi) pathway[22,23] that is similar to the noncanonical miR-451 processing pathway.[24–26] To inhibit miR-210, an antisense oligonucleotide (antimiR) approach targeting miR-210 was used.[27]

Delivery of oligonucleotides to tissues other than the liver remains a significant hurdle to the development of effective nucleic acid-based therapeutics.[28] Because of the nature of wound sites, we have opted for a localized rather than systemic approach to delivery of the RNAi and antisense oligonucleotides. Using a novel layer-by-layer (LbL) technology, we formulated the oligonucleotides into a thin film polymer coating atop a nylon woven mesh.[29,30] This

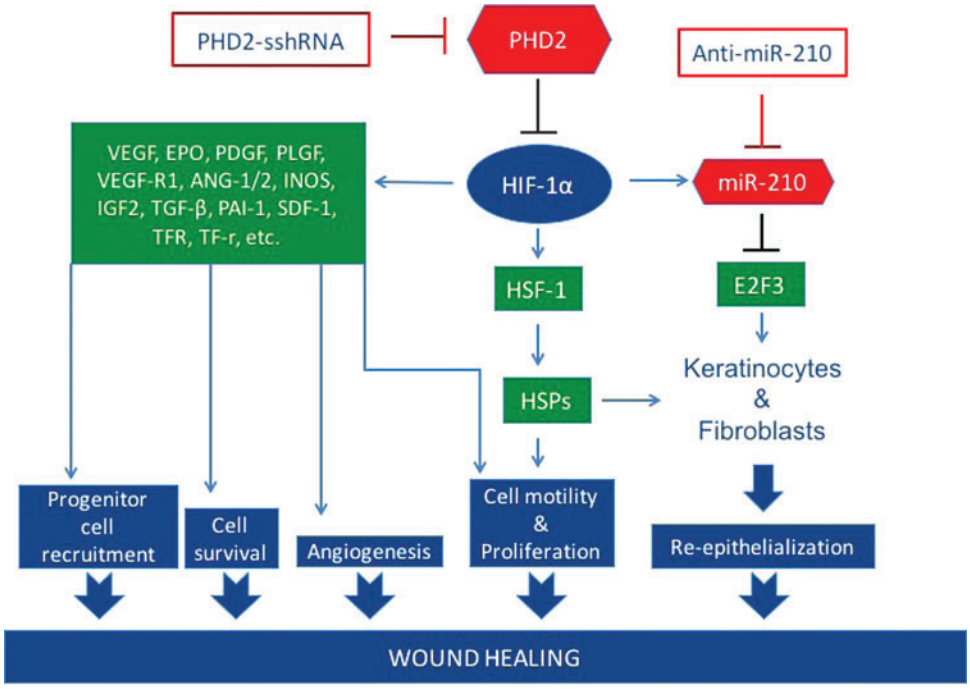

FIG. 1. Pathways involved in the wound healing process regulated by HIF-1α together with the molecular targets for inhibition. PHD2 is targeted for inhibition with an sshRNA, and miR-210 is targeted for inhibition by an antisense oligonucleotide (antimiR). HIF-1α, hypoxia-inducible factor-1α; PHD2, prolyl hydroxylase domain-containing protein 2; sshRNA, short synthetic hairpin RNA.

formulation provides slow release of the encapsulated oligonucleotides into the wound bed over the course of 7–10 days. Previous studies have shown that siRNAs delivered by this method are taken up by cells.[29,30]

In this study, we report the identification of an sshRNA (SG404) and an antimiR (SG608), both chemically modified, that potently inhibit PHD2 and miR-210, respectively, and promote keratinocyte growth and mobility *in vitro*. When these RNAs were formulated into LbL-coated dressings and applied to full-thickness excisional wounds in diabetic mice, time to wound closure was significantly reduced and increased expression was seen in markers of neovascularization and proliferation in the wound area. These effects were observed with each inhibitor alone and with enhanced effect when they were combined in a single LbL formulation.

Materials and Methods

In vitro *target knockdown assays*

Cells (primary keratinocytes [NHEK], HaCaT, or NIH-3T3) were seeded at 23,000 cells/well in 96-well or at 30,000 cells/well in 48-well plates 1 day before transfection. Triplicate transfections of PHD2 sshRNAs and miR-210 antimiRs at various concentrations along with nonspecific control (NSC) sshRNAs and antimiRs were performed using HiPerFect (Qiagen) or RNAiMAX (Invitrogen, Carlsbad, CA) following the manufacturer's instructions. Total RNA was extracted using the RNeasy 96 or miRNeasy kits (Qiagen) 48 h later. PHD2 messenger RNA (mRNA) and miR-210 levels were quantified by real-time quantitative polymerase chain reaction (RT-qPCR) on a 7500 Fast RT-PCR system (Applied Biosystems; see Supplementary Methods [Supplementary Data are available online at www.liebertpub.com/tea] for details). mRNA and miRNA levels were quantified using the $\Delta\Delta$Ct method,[31] normalizing to GAPDH and sno234, respectively. Dose curves were plotted and IC_{50} values were computed using GraphPad Prism software.

HIF-1α reporter assay

293FT cells were seeded at 30,000 cells/well in a 96-well plate 1 day before transfection. One hundred nanograms of HIF firefly luciferase (fLuc) reporter plasmid (Cignal HIF reporter Luc Kit; SABiosciences), a control plasmid (rLuc), and 12 nM sshRNA were transfected in triplicate using Lipofectamine2000 (Lipo2K; Invitrogen) according to the manufacturer's instructions. Forty-eight hours later, the cells were lysed in 150 μL lysis buffer (Promega). fLuc and rLuc levels were measured using a TR 717 Microplate Luminometer (Applied Biosystems) and induction of HIF was calculated.

Biosensor assay

An miR-210 biosensor plasmid (pSG247) was prepared, and the biosensor assay to measure the activity of antimiR targeting miR-210 was performed as described in Supplementary Methods.

Scratch assay

HaCaT cells were seeded at 400,000 cells/well into 12-well plates 1 day before transfection. sshRNAs and antimiRs (final concentration, 30 nM each) were transfected using HiPerFect (Qiagen) following the manufacturer's protocol. Twenty-four hours post-transfection, the medium was changed to 0.5% fetal bovine serum and two scratches were drawn per well using a P20 pipette tip. Photographs and measurements across the cell-free scratches were taken immediately after scratching and at 24, 48, and 72 h post-transfections. Because the initial scratches were not of uniform width, we analyzed by calculating the percent scratch width closure at each time point relative to the initial scratch width.

Proinflammatory cytokine detection in vitro

Assessment of proinflammatory cytokine levels on transfection of PHD2 sshRNAs and miR-210 antimiRs into MRC-5 lung fibroblast cells was performed exactly as described in Dallas *et al.*[20]

Formulation of oligonucleotides for in vivo *delivery*

sshRNA and antimiR oligonucleotides were formulated into a thin film coating assembled by LbL deposition[32] onto the surface of a woven nylon wound dressing (Tegaderm™; 3M, St. Paul, MN) by LayerBio, Inc. (See the Results section for a general description of the method.) Four different wound dressing samples were generated for *in vivo* testing incorporating the following oligonucleotides: (1) PHD2-specific sshRNA SG404, (2) miR-210 antimiR SG608, (3) SG404 combined with SG608, and (4) NSC RNA (SG221c). Oligonucleotide loading within the thin film coating is approximated to be 25 μg/cm^2. The RNA-coated dressing was applied directly to the wound bed.

Animals

All mice were housed in the Stanford University Veterinary Service Center in accordance with the National Institutes of Health (NIH) and institution-approved animal care guidelines. All procedures were approved by the Stanford Administrative Panel on Laboratory Animal Care.

Wound model

Fourteen-week-old male C57BL/6 db/db mice (BKS.Cg-Dock7m +/+ Leprdb/J) were purchased from Jackson Laboratory (Bar Harbor, ME). A stented excisional wound healing model was used as previously described.[33] Briefly, after induction of anesthesia, all hair on the dorsum of the mice was removed using a shaver and depilatory cream. Two excisional wounds were then generated on the dorsum of each mouse using a 6 mm disposable biopsy punch (Integra). To prevent contraction, each wound was splinted open using a silicone ring (Grace BioLabs) with outer and inner diameters of 16 and 10 mm, respectively, attached with cyanoacrylate glue (Krazy Glue, West Jefferson, OH) and 6-0 black nylon sutures (Ethicon).

Administration of LbL-formulated oligonucleotides

One day after wounding, oligonucleotide formulated dressings were cut with a 6 mm disposable biopsy punch and

placed into the wound bed. Treatments were secured in place by an occlusive adherent dressing (Tegaderm; 3M). As the wound healed and closed, each patch was carefully removed and trimmed to fit the wound area.

Wound analysis

Dressings were removed and digital photographs were taken of each wound on the day of surgery and every other day until closure. The analysis of the wound area was performed by measuring the wound area normalized to the inner diameter of the silicone ring. The ratio of the wound area for all time points to initial wound area on the day of surgery was measured and calculated by a blinded observer using ImageJ (NIH, Bethesda, MD).

Histological analysis

Wounds were harvested with a 2 mm ring of unwounded skin from euthanized mice. The wounds were then bisected into hemispherical pieces. The pieces of skin tissue were fixed overnight in 4% paraformaldehyde followed by a serial dehydration in ethanol and paraffin embedding. Five-micron-thick paraffin sections were prepared from wound tissue harvested on days 4, 7, and on wound closure after treatment with LbL-oligonucleotide formulations. Day 4 sections were stained for CD31 (Abcam, Cambridge, MA) and Ki67 (Abcam). Day 7 sections were stained for von Willebrand factor (vWF; antibody No. 7356; EMD Millipore, St. Louis, MO). Healed wounds were stained with hematoxylin and eosin (H&E) and trichrome. Nuclei were stained with DAPI (EMD Millipore). Quantification was performed using ImageJ.

Protein analysis

Wound tissue was harvested after euthanasia on days 2 and 4 post-treatment application similarly to the histology sections except that the remaining hemispherical sections were bisected and designated for protein or RNA analysis. Samples for protein analysis were snap-frozen in microcentrifuge tubes and stored at −80°C until testing. The tissue samples were then homogenized (KINEMATICA polytron; Thermo Fisher Scientific, Waltham, MA) and protein was extracted using RIPA buffer (Sigma-Aldrich, St. Louis, MO) and Halt protease inhibitor cocktail (Thermo Fisher Scientific). The isolated soluble protein extract was then analyzed for VEGF protein levels (ELISA Quantikine kits; R&D Systems, Inc., Minneapolis, MN).

Statistical analysis

Statistical analysis was performed using an unpaired Student's *t*-test. Values are presented as mean ± standard error of the mean (SEM). *p*-values <0.05 were considered statistically significant.

Results

Identification of potent sshRNA inhibitors of human and mouse PHD2

We iteratively designed and screened for potency sshRNA inhibitors of both human and mouse versions of PHD2 based on target site prediction algorithms and previously reported siRNA sequences[8–10,34] and then performed sequence walking around effective target sites. All sshRNAs were designed to have left-hand loop orientation, 19-bp stems, and a 2-nt loop, a structural design that was previously shown to be effective both *in vitro*[22,23,35] and *in vivo*.[20,21] Each sshRNA was screened for the ability to inhibit PHD2 expression in cell culture, resulting in the identification of SG302 (human) and SG402 (mouse) as the most potent inhibitors of PHD2 expression. Dose/response curves (Fig. 2A, B) show highly potent knockdown of PHD2 mRNA (IC_{50} = 3.5 pM for SG302, 29 pM for SG402).

Chemical stabilization of sshRNAs and antimiRs

Chemical modification of RNA oligonucleotides serves both to enhance biostability by increasing resistance to degradation by serum nucleases and to mitigate potential undesirable immune stimulatory effects. Chemically modified versions of SG302 and SG402 (SG302m1 and SG404, respectively) containing 2′-OMe modifications at select positions in the sense (or passenger) strand sequence and loop nucleotides as described in Dallas *et al.*[20] and Ge *et al.*[35] were synthesized and their ability to inhibit PHD2 mRNA expression was examined in cell culture. The inhibitory dose curves are shown in Figure 2A and B alongside their unmodified counterparts, confirming that these modified oligonucleotides retain high potency for their respective targets ([SG302m1] IC_{50}, 14 pM; [SG404] IC_{50}, 44 pM). A modified 5′-Rapid Amplification of cDNA (complementary DNA) Ends (5′-RACE) assay was performed to confirm that PHD2 mRNA was cleaved at the predicted site of RNAi-mediated cleavage (Supplementary Fig. S1).

Identification of a potent antisense inhibitor (antimiR) of miRNA-210

Under normoxic conditions, miR-210, a key miRNA upregulated by HIF-1α, has been shown to negatively impact wound healing by inhibiting keratinocyte growth and proliferation.[18] By identifying an effective antimiR to miR-210, we aimed to abrogate the negative effects of miR-210 upregulation on stabilization of HIF-1α. AntimiRs were screened for potency in cell culture using a luciferase reporter biosensor (pSG247) assay. In this assay, rLuc is derepressed to an extent that correlates with antimiR efficacy. We tested a variety of chemical modification patterns, including various combinations of 2′-OMe, locked nucleic acid, and phosphorothioates (data not shown), with and without N,N-diethyl-4-(4-nitronaphthalen-1-ylazo)-phenylamine (''ZEN'') moieties at both the 5′- and 3′-ends. The ZEN modification increases the T_m for target binding and increases stability toward serum and cytoplasmic endonucleases and exonucleases.[36] One antimiR (SG608), comprising all 2′-OMe-substituted residues with ZEN-modified ends, proved to be particularly potent in cell culture. SG608-transfected cells exhibited derepression of rLuc expression by up to threefold compared with cells lacking antimiR (Fig. 2C).

Simultaneous and specific inhibition of PHD2 and miR-210

Having demonstrated the specific inhibition of miR-210 and PHD2 targets with each inhibitor alone, we also tested

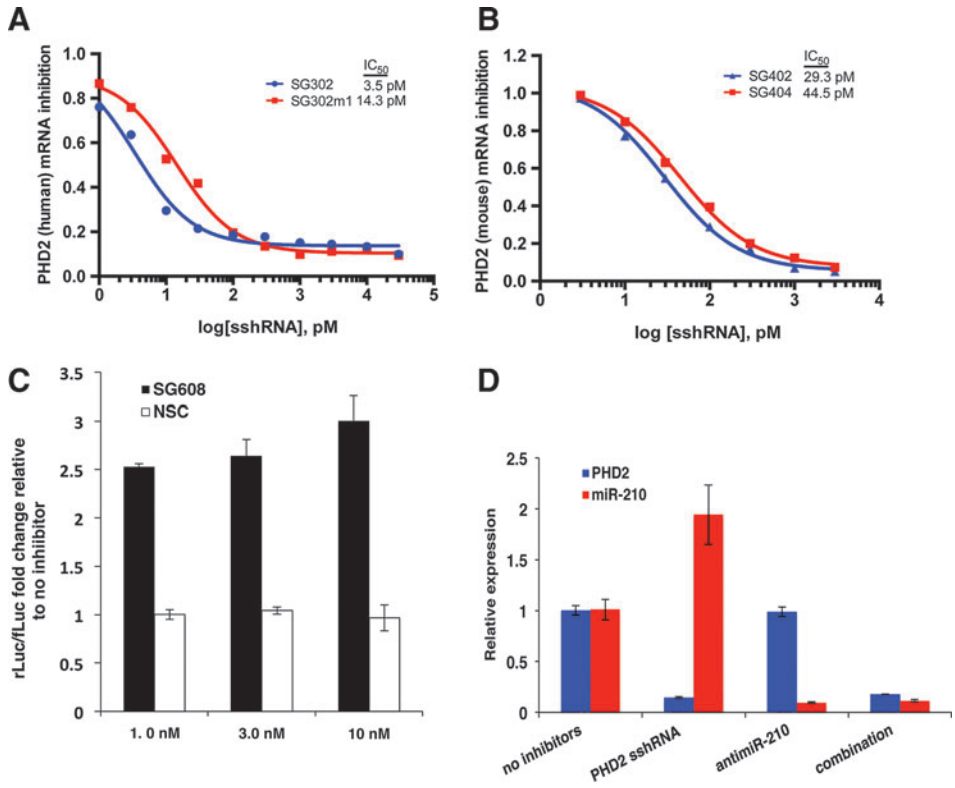

FIG. 2. Inhibition of PHD2 and miR-210. **(A, B)** Dose/response curves of PHD2 inhibition by sshRNAs targeting human **(A)** and mouse **(B)** PHD2 mRNAs. Efficacies of unmodified and 2′-OMe-modified sshRNAs (SG302 vs. SG302m (human) and SG402 vs. SG404 (mouse)) are shown over the indicated concentration range. Total RNA was isolated 48 h after transfections in NHEK cells (human) and NIH-3T3 (mouse). PHD2 transcripts were quantified by RT-qPCR using the $\Delta\Delta C_t$ method, normalizing to GAPDH. Quantification is expressed as fold-inhibition relative to cells that were not transfected with inhibitors. **(C)** Luciferase biosensor assay to measure inhibition of miR-210 by antimiRs. Derepression of rLuc signal shows specific activity of miR-210-targeting antimiR SG608 relative to NSC control antimiR. **(D)** Specific inhibition of PHD2 and miR-210 by sshRNA and antimiR in cell culture. qPCR analysis of PHD2 transcript levels and miR-210 levels (*red*) in keratinocytes (HaCaT) 48 h after transfection with PHD2 sshRNA, miR-210 antimiR, or a combination of both. Quantification is expressed as fold-change relative to cells that were not transfected with inhibitors. mRNA, messenger RNA; NSC, nonspecific control; RT-qPCR, real-time quantitative polymerase chain reaction.

them in combination in HaCaT cells (Fig. 2D) and monitored for effects on both PHD2 and miR-210 48 h after transfection by RT-qPCR. When PHD2 sshRNAs were transfected alone, PHD2 mRNA levels were reduced by 85%, while miR-210 levels were increased twofold, as expected. In contrast, when anti-miR-210 was transfected alone, PHD2 mRNA levels were unaffected, while miR-210 levels were strongly reduced. Finally, in cells cotransfected with both PHD2-sshRNA and antimiR-210, the PHD2 and miR-210 levels were reduced to the same extent as with each inhibitor alone.

Inhibition of PHD2-sshRNA results in increased HIF-1α expression

The efficacy of PHD2-sshRNA in upregulating HIF-1α was assessed by using a luciferase reporter assay. Forty-eight hours after cotransfection of the reporter plasmids and either PHD2-specific sshRNA (SG302) or NSC sshRNA (SG221c), we confirmed that SG302 was able to upregulate HIF-1α (Fig. 3A). We further validated this result by Western blot, where we observed a 1.8-fold increase in HIF-1α levels relative to controls (Supplementary Fig. S2A).

Demonstration of enhanced keratinocyte growth with PHD2 and miR-210 inhibitors

To measure cell migration, we performed a scratch assay with HaCaT cells as described in Kioka *et al.*[37] Figure 3B and Supplementary Figure S2B show that keratinocytes narrowed the width of the cell-free region much more rapidly when transfected with the active anti-miR-210 and PHD2 sshRNAs than with PHD2 sshRNA alone or NSCs ($p = 0.007$, 0.001, and 0.003 for 24, 48, and 72 h time points, respectively).

Chemically modified oligonucleotides do not induce proinflammatory cytokines, are not cytotoxic, and have improved biostability

Unmodified RNAs are capable of inducing the undesired expression of proinflammatory cytokines,[38] but this off-target effect can be avoided by incorporating 2′-OMe nucleotides.[35,39] We evaluated the cytokine-inducing ability of sshRNAs and antimiRs with and without chemical modifications in human fetal lung fibroblast (MRC-5) cells, which

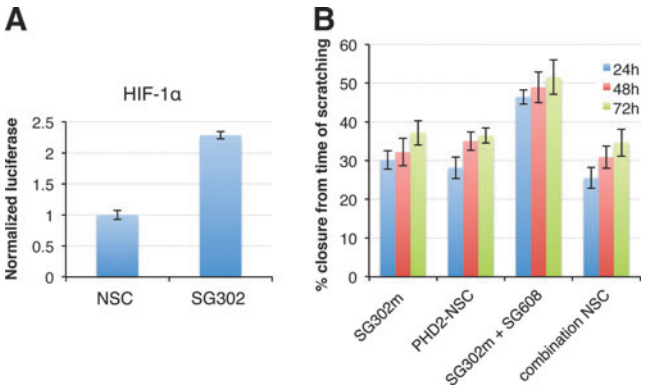

FIG. 3. Verification of functional activities induced by inhibition of PHD2 and miR-210. **(A)** Induction of HIF-1α by human PHD2-targeting sshRNA SG302 by transactivation of a PHD2-dependent luciferase reporter. **(B)** PHD2 and miR-210 inhibitors increase keratinocyte migration in scratch assay. Percent scratch closure is shown at 24, 48, and 72 h after human HaCaT keratinocytes were transfected with the indicated inhibitors at 10 nM final concentration. SG302m is chemically modified PHD2 sshRNA, PHD2-NSC is a scrambled NSC sshRNA, SG302m+SG608 is cotransfected PHD2 sshRNA and N,N-diethyl-4-(4-nitronaphthalen-1-ylazo)-phenylamine (ZEN)-modified miR-210 antimiR-210, combination NSC is cotransfection with NSC sshRNA and NSC antimiR.

are known to be sensitive to immunostimulatory oligonucleotides[40] and can be activated by cytosolic RNA through RIG-I-like receptors. Poly I:C, a well-known inducer of proinflammatory cytokines, was used as a positive control. Since the oligonucleotides used in this study have maximum target gene knockdown at concentrations of 0.3–10 nM, we used 20 nM oligonucleotides (final concentration) to examine their abilities to upregulate interferon (IFN) expression within the likely limits of a therapeutic dose. Unmodified sshRNAs and antimiRs (SG302 and SG601, respectively) were investigated along with their modified counterparts (SG302m1 and SG608) (Table 1). As anticipated, none of these oligonucleotides shows significant induction of inflammatory cytokines. In addition, we confirmed that the modified sshRNAs and antimiRs are noncytotoxic and do not decrease cell viability with respect to control transfections (Supplementary Fig. S3).

One of the factors that govern the pharmacokinetics of oligonucleotide-based drugs is their sensitivity to nucleases

Table 1. Immunostimulatory Properties of Short Synthetic Hairpin RNAs and AntimiRs

		TNF-α	*IL-6*
sshRNA	No inhibitor	1.00 ± 0.02	1.02 ± 0.14
	PolyI:C	263.03 ± 6.41	1427.51 ± 31.32
	SG302	0.49 ± 0.02	0.68 ± 0.13
	SG302m	2.25 ± 0.43	1.01 ± 0.10
antimiR	No inhibitor	1.00 ± 0.34	1.02 ± 0.25
	Poly I:C	6494.43 ± 434.01	528.38 ± 24.93
	SG601	0.95 ± 0.50	1.21 ± 0.40
	SG608	1.32 ± 0.39	0.97 ± 0.00

sshRNA, short synthetic hairpin RNA.

found in serum. sshRNAs without chemical modification are susceptible to degradation in 10% human serum despite being largely double-stranded. We found that stability increased on 2′-*O*Me modification at alternate nucleotides of the sense strand and each nucleotide in the UU loop (SG404 vs. SG402, Supplementary Fig. S4). SG608, which is a fully modified single-stranded oligonucleotide, was shown to be extremely stable in 10% human serum, with $t_{1/2} > 96$ h.

Oligonucleotide formulation for in vivo *delivery*

SG404 and SG608 were formulated using LbL technology (LayerBio, Inc.). LbL is a technique through which a thin film is generated based on the alternating adsorptions of two or more polymers or other species on the basis of complementary interactions (charge, hydrogen bonding).[41] For this study, negatively charged nucleic acids (SG404, SG608, and/or control oligonucleotides) were coassembled via LbL with positively charged polymers into a thin multilayer coating onto the surface of a nylon woven dressing (Tegaderm) following previously demonstrated methods.[30] Briefly, the layers are applied by alternately immersing the substrate into reservoirs containing solutions of positively and negatively charged polymers, respectively, rinsing after each immersion. The RNA-coated dressing is applied directly to the wound bed and biodegrades over 7–10 days with a sustained release of sshRNA-polycation polyplexes.

To confirm effective delivery of these RNAs *in vivo*, a fluorescent-tagged version of PHD2 sshRNA (SG405) formulated by LbL was applied to full-thickness excisional wounds in db/db mice (Supplementary Methods). The wounds were imaged 2 and 6 days after application (Fig. 4A) and fluorescence intensity was quantified (Fig. 4B). The results showed uptake of SG405-sshRNA into cells in the dermal layer of the wound area at both time points.

LbL delivery of SG404 and SG608 improves wound healing

To assess the activity of the therapeutic oligonucleotides, LbL-formulated SG404, SG608, or a combination of SG404/SG608 was applied to full-thickness excisional wounds[33] ($n = 8$) in diabetic mice 1 day postwounding and compared with both an untreated control group and group treated with an LbL-formulated NSC sshRNA. As shown in Figure 4C–E, SG404- and SG608-treated wounds closed 4 days faster than untreated control wounds: on average, 17.25 days after wounding versus 21.25 days [$p_{(\text{SG404 vs. control})} = 0.002$ and $p_{(\text{SG608 vs. control})} = 0.0006$]. Wounds treated with both SG404 and SG608 simultaneously closed 4.75 days faster (SEM 0.32) than untreated control. At earlier time points, SG404, SG608, and the combination show a similar rate of closure (51%, 55%, 56%, respectively, vs. 40% control at day 10), but after 2 weeks, the combination treatment results in accelerated wound closure over the individual treatments (86%, 84%, 95% vs. 68% control at day 16) (Fig. 4C). LbL-formulated NSC-treated wounds closed 1 day faster than untreated control wounds, suggesting that the dressing itself may partially contribute to the accelerated wound closure. Nevertheless, the specific treatments SG404, SG608, and combined SG404/SG608 still closed significantly faster than LbL-NSC ($p = 0.01$, 0.006, and 0.0003, respectively).

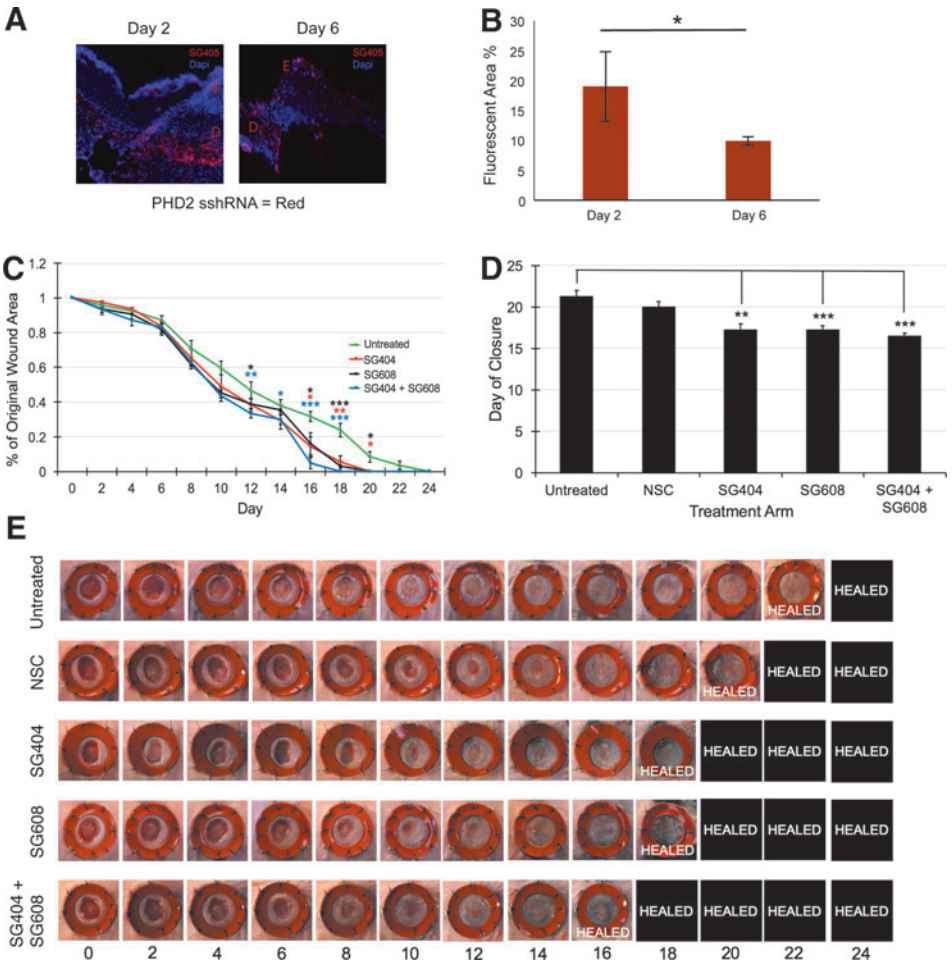

FIG. 4. *In vivo* delivery and efficacy of therapeutic RNAs. **(A)** Delivery of PHD2-sshRNAs using LbL formulation. Uptake into the dermal layer at days 2 and 6 of a fluorescent-tagged version of SG404 (SG405, *red*). Nuclei are stained with DAPI (*blue*). **(E)** Epidermis, **(D)** dermis. **(B)** Quantification of fluorescence uptake. **(C–E)** PHD2 and miR-210 inhibition improves wound healing in diabetic murine wounds. **(C)** Time course of wound closure showing significantly faster closure with SG404, SG608, and combination treatments compared to the untreated control. **(D)** Results from **(C)** replotted to show time to closure. **(E)** Representative images of full-thickness excisional wounds treated with therapeutic RNAs and controls. Photos were taken on day 0 and every 2 days thereafter (*horizontal* axis) until closure was complete. The *orange rings* are silicone splints to prevent wound contraction. $*p<0.05$; $**p<0.01$; $***p<0.001$. LbL, layer-by-layer.

Trichrome and H&E staining of remodeled wound beds demonstrated increased collagen deposition and appendage remodeling, particularly in the SG608 treatment. We observed a more defined dermal layer and increased collagen in the combination treatment (Supplementary Fig. S5). In all of the specific treatment groups, there was an increase in the average number of appendages per wound versus controls: SG404 (27.6 ± 4.3), SG608 (38.4 ± 18.2), SG404+SG608 (40.6 ± 13.6) versus untreated (16.8 ± 4.3) and NSC (16.4 ± 6.4).

PHD2-sshRNA and antimiR-210 treatments enhance neovascularization and cellular proliferation

We then looked at how each treatment, both alone and in combination, affected neovascularization with CD31 staining. Histological samples obtained at day 4 after the start of treatment showed enhanced neovascularization, with the combination treatment showing the greatest enhancement, over controls (Fig. 5A, red staining). Samples were also stained for Ki-67, a marker for proliferation. Consistent with accelerated closure of wounds receiving oligonucleotide treatment, there was an increase in Ki-67 staining (Fig. 5B, red staining). A significant increase in neovascularization was also observed at day 7 by vWF staining (Supplementary Fig. S6) for SG404-treated wounds over NSC and untreated control wounds in a separate experiment in which only the effect of SG404 was examined.

Molecular analysis

Analysis of RNA levels in total RNA isolated from wound tissue harvested day 4 after start of treatment showed a reduction in miR-210 levels only in treatment groups in which SG608 was applied, which also confirms delivery of the antimiR to the cells in the wound area (Fig. 5C).

Analysis of VEGF and SDF-1 levels in wound tissue harvested on day 2 showed a significant ($p<0.05$) increase in the group treated with SG404 alone (Supplementary Fig. S7), as expected, based on the induction of VEGF by HIF-1α (Fig. 1). Tissue harvested on day 4 (Fig. 5D) showed a similar result for SG404 alone. However, the two groups treated with SG608 (alone or combined with SG404) showed no change in VEGF levels over controls, consistent with the angiogenesis-promoting effects of miR-210, which at this time point apparently counter the VEGF-inducing effects of SG404.

Discussion

Chronic diabetic wounds, particularly pressure ulcers, affect 2.5 million people in the United States and cost the healthcare system an estimated $11.6 billion annually.[5,42,43] While interventions exist,[44–48] current treatments are only moderately effective.[49] Critical cellular and molecular pathways responsible for normal wound healing, including the

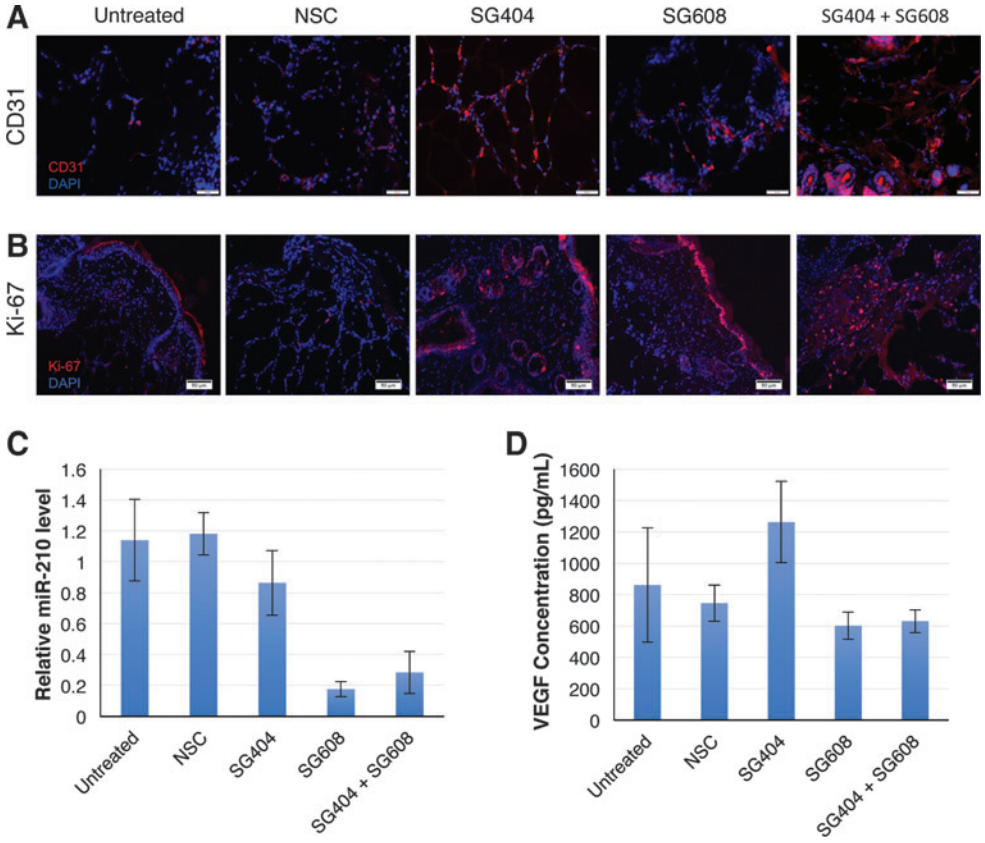

FIG. 5. Neovascularization and cell proliferation are improved on inhibition of PHD2 and miR-210 in diabetic murine wounds. **(A)** Images taken on day 4 of treatment show improved neovascularization at the wound periphery. The combination treatment showed greatest improvement compared to untreated and NSCs. *Red*: CD-31, *blue*: DAPI. **(B)** Increased cell proliferation was observed in the SG404 and SG608 groups. *Red*: Ki-67, *blue*: DAPI. **(C)** Verification of specific knockdown of miR-210 by SG608 in tissue isolated at day 4. **(D)** Enhancement of VEGF protein levels (ELISA) with PHD2 knockdown (SG404) at day 4. ELISA, enzyme-linked immunosorbent assay; VEGF, vascular endothelial growth factor.

hypoxia response regulated by HIF-1α, are impaired in diabetes.[50–60] Diabetes-related defects have lower levels of signaling that impair neovascularization, fibroblast function, and wound healing.[12,50,51,61–68] The effectiveness of introducing growth factors has been limited, in part, by the presence of high levels of proteases in the wound environment. Unlike proteins, RNAs can be chemically stabilized against degradative enzymes without compromising their functional activity. Thus, they represent a promising class of targeted therapeutic agents for this challenging condition.

In this study, we examined the use of chemically modified RNAs as therapeutic agents for treating chronic diabetic wounds by targeting the HIF-1α wound healing pathway in db/db mice. In particular, SG404, a chemically modified sshRNA targeting PHD2, and SG608, a modified anti-miR-210, were each shown to significantly accelerate wound closure in full-thickness punch wounds, alone and in combination. A key element in the treatment was the use of LbL technology to deliver high local concentrations of therapeutic RNA.

Several lines of evidence presented here support the modes of action as outlined in Figure 1, with SG404 inhibiting PHD2 and stabilizing HIF-1α, and SG608 inhibiting miR-210 and abrogating its negative effects on keratinocyte growth and mobilization. First, irrelevant sshRNAs of the same structural design as SG404 have little or no effect (Figs. 3A and 4C, E). Second, SG404 was shown to knock down PHD2 and upregulate levels of HIF-1α in keratinocytes, consistent with the role of PHD2 in destabilizing HIF-1α (Fig. 3B and Supplementary Fig. S2B). Similarly, SG608 was shown to derepress targets of miR-210 *in vitro* (Fig. 2C) and knock down levels of miR-210 in the wound margins *in vivo* (Fig. 5C). Third, factors downstream of HIF-1α that are involved in wound healing (VEGF, SDF-1) are upregulated in the wound margins treated with SG404 alone (Fig. 5D and Supplementary Fig. S7). Fourth, transfection of SG404 and SG608 into HaCaT cells results in increased growth and mobilization in scratch assays (Fig. 3B and Supplementary Fig. S2B). Finally, staining for vWF and CD31 shows increased angiogenesis at days 4 and 7 and staining for Ki-67 shows increased proliferation at day 4 post-treatment initiation (Fig. 5 and Supplementary Fig. S6).

The effectiveness of inhibiting miR-210 alone suggests that this miRNA may play a significant role in chronic wounds. miR-210 is upregulated on binding of HIF-1α to a hypoxia responsive element (HRE) in the promoter of miR-210,[69] and hence its levels are elevated when HIF-1α is stabilized. Biswas *et al.*[18] reported that levels of miR-210 are elevated in ischemic cutaneous wounds and are associated with impairment of keratinocyte growth and re-epithelialization. In addition, miR-210 is implicated in a number of other processes related to wound healing, including angiogenesis, mitochondrial metabolism, and oxidative stress.[2] While its role in promoting angiogenesis is consistent with a positive role in wound healing, the other processes it promotes tend to be detrimental. This is particularly true in the case of keratinocyte proliferation, which miR-210 inhibits by targeting E2F3 and thereby blocking entry into S phase and initiation of DNA replication. The suppression by miR-210 of mitochondrial respiration, while allowing cells to survive longer under hypoxic conditions, reduces available adenosine triphosphate (ATP), which is required in abundance for wound healing.

Our results support the concept that inhibition of miR-210 and hence reduction of the above detrimental influences of miR-210 on wound healing more than compensate for the proangiogenic effects of this miRNA. Indeed, moderate impairment of angiogenesis alone does not necessarily retard normal wound healing.[70] The observation that anti-miR-210 appears to counter the upregulation of VEGF seen on knockdown of PHD2 at day 4 is interesting in light of the increased extent of neovascularization seen at this time point (Fig. 5D). It may be that other proangiogenic influences make up for the reduction in VEGF, or that VEGF acts at an earlier time point (Supplementary Fig. S7).

The method of RNA delivery used in this study, an LbL coating of RNA on Tegaderm mesh, has important advantages as a practical treatment approach. Electrostatic complexation and the solid-phase nature of the LbL film limit the exposure of nucleic acids to environmental conditions, affording long-term storage stability that is important for stocking in clinics, including in resource-challenged settings. Importantly, LbL formulations allow for topical application of therapeutic oligonucleotides, providing high local concentrations spread over several days with very low systemic exposure.

While both RNAi[10,13,14,30] and antisense[18] oligonucleotides have been reported previously for the ability to accelerate wound healing individually, to our knowledge this is the first study to combine both modalities. The efficacy illustrates the potential of combining therapeutic RNAs targeting both mRNA and miRNA in a single formulation with potential superiority to either modality on its own.

Acknowledgments

We thank Yujin Park for assistance with tissue processing and staining and Mark Behlke for providing the ZEN-modified RNAs. Funding for this project has been provided by the NIH (R43GM101725 [B.H.J.], R44GM101725 [B.H.J.], and R01-DK074095 [G.C.G.]).

Disclosure Statement

A.D., H.I., and B.H.J. are employees and shareholders of SomaGenics; J.M. is a consultant for SomaGenics, the Gurtner laboratory (A.T., C.A.B., M.R., K.E., J.A.B., N.K., Z.A.S.-B., G.C.G.), was a recipient of a subcontract from SomaGenics of NIH grant R44GM101725; and A.W. and K.J.M. are employees and shareholders of LayerBio, Inc. S.J. has nothing to disclose.

References

1. CDC. National Diabetes Statistics Report. 2017. www.cdc.gov/diabetes/pdfs/data/statistics/national-diabetes-statistics-reportpdf (last accessed June 14, 2018).
2. Sen, C.K., Gordillo, G.M., Roy, S., *et al.* Human skin wounds: a major and snowballing threat to public health and the economy. Wound Repair Regen **17,** 763, 2009.
3. Singh, N., Armstrong, D.G., and Lipsky, B.A. Preventing foot ulcers in patients with diabetes. JAMA **293,** 217, 2005.
4. Lavery, L.A., Peters, E.J., and Armstrong, D.G. What are the most effective interventions in preventing diabetic foot ulcers? Int Wound J **5,** 425, 2008.
5. Rice, J.B., Desai, U., Cummings, A.K., Birnbaum, H.G., Skornicki, M., and Parsons, N.B. Burden of diabetic foot ulcers for medicare and private insurers. Diabetes Care **37,** 651, 2014.
6. Izumi, Y., Satterfield, K., Lee, S., Harkless, L.B., and Lavery, L.A. Mortality of first-time amputees in diabetics: a 10-year observation. Diabetes Res Clin Pract **83,** 126, 2009.
7. Elson, D.A., Ryan, H.E., Snow, J.W., Johnson, R., and Arbeit, J.M. Coordinate up-regulation of hypoxia inducible factor (HIF)-1alpha and HIF-1 target genes during multi-stage epidermal carcinogenesis and wound healing. Cancer Res **60,** 6189, 2000.
8. Berra, E., Benizri, E., Ginouves, A., Volmat, V., Roux, D., and Pouyssegur, J. HIF prolyl-hydroxylase 2 is the key oxygen sensor setting low steady-state levels of HIF-1alpha in normoxia. EMBO J **22,** 4082, 2003.
9. Schultz, K., Murthy, V., Tatro, J.B., and Beasley, D. Prolyl hydroxylase 2 deficiency limits proliferation of vascular smooth muscle cells by hypoxia-inducible factor-1{alpha}-dependent mechanisms. Am J Physiol Lung Cell Mol Physiol **296,** L921, 2009.
10. Wu, S., Nishiyama, N., Kano, M.R., *et al.* Enhancement of angiogenesis through stabilization of hypoxia-inducible factor-1 by silencing prolyl hydroxylase domain-2 gene. Mol Ther **16,** 1227, 2008.
11. Huang, J., Zhao, Q., Mooney, S.M., and Lee, F.S. Sequence determinants in hypoxia-inducible factor-1alpha for hydroxylation by the prolyl hydroxylases PHD1, PHD2, and PHD3. J Biol Chem **277,** 39792, 2002.
12. Thangarajah, H., Yao, D., Chang, E.I., *et al.* The molecular basis for impaired hypoxia-induced VEGF expression in diabetic tissues. Proc Natl Acad Sci U S A **106,** 13505, 2009.
13. Wetterau, M., George, F., Weinstein, A., *et al.* Topical prolyl hydroxylase domain-2 silencing improves diabetic murine wound closure. Wound Repair Regen **19,** 481, 2011.
14. Zhang, X., Yan, X., Cheng, L., *et al.* Wound healing improvement with PHD-2 silenced fibroblasts in diabetic mice. PLoS One **8,** e84548, 2013.
15. Chan, Y.C., Banerjee, J., Choi, S.Y., and Sen, C.K. miR-210: the master hypoxamir. Microcirculation **19,** 215, 2012.
16. Ivan, M., and Huang, X. miR-210: fine-tuning the hypoxic response. Adv Exp Med Biol **772,** 205, 2014.
17. Ivan, M., Harris, A.L., Martelli, F., and Kulshreshtha, R. Hypoxia response and microRNAs: no longer two separate worlds. J Cell Mol Med **12,** 1426, 2008.
18. Biswas, S., Roy, S., Banerjee, J., *et al.* Hypoxia inducible microRNA 210 attenuates keratinocyte proliferation and impairs closure in a murine model of ischemic wounds. Proc Natl Acad Sci U S A **107,** 6976, 2010.
19. Chan, S.Y., and Loscalzo, J. MicroRNA-210: a unique and pleiotropic hypoxamir. Cell Cycle **9,** 1072, 2010.
20. Dallas, A., Ilves, H., Shorenstein, J., *et al.* Minimal-length synthetic shRNAs formulated with lipid nanoparticles are potent inhibitors of hepatitis C virus IRES-linked gene expression in mice. Mol Ther Nucleic Acids **2,** e123, 2013.
21. Ma, H., Dallas, A., Ilves, H., *et al.* Formulated minimal-length synthetic small hairpin RNAs are potent inhibitors of hepatitis C virus in mice with humanized livers. Gastroenterology **146,** 63, 2014.
22. Ge, Q., Ilves, H., Dallas, A., *et al.* Minimal-length short hairpin RNAs: the relationship of structure and RNAi activity. RNA **16,** 106, 2010.
23. Dallas, A., Ilves, H., Ge, Q., *et al.* Right- and left-loop short shRNAs have distinct and unusual mechanisms of gene silencing. Nucleic Acids Res **40,** 9255, 2012.

24. Cheloufi, S., Dos Santos, C.O., Chong, M.M., and Hannon, G.J. A dicer-independent miRNA biogenesis pathway that requires Ago catalysis. Nature **465,** 584, 2010.
25. Cifuentes, D., Xue, H., Taylor, D.W., *et al.* A novel miRNA processing pathway independent of Dicer requires Argonaute2 catalytic activity. Science **328,** 1694, 2010.
26. Yang, J.S., Maurin, T., Robine, N., *et al.* Conserved vertebrate mir-451 provides a platform for Dicer-independent, Ago2-mediated microRNA biogenesis. Proc Natl Acad Sci U S A **107,** 15163, 2010.
27. Lennox, K.A., and Behlke, M.A. Chemical modification and design of anti-miRNA oligonucleotides. Gene Ther **18,** 1111, 2011.
28. Haussecker, D. Current issues of RNAi therapeutics delivery and development. J Control Release **195,** 49, 2014.
29. Castleberry, S., Wang, M., and Hammond, P.T. Nanolayered siRNA dressing for sustained localized knockdown. ACS Nano **7,** 5251, 2013.
30. Castleberry, S.A., Almquist, B.D., Li, W., *et al.* Self-assembled wound dressings silence MMP-9 and improve diabetic wound healing in vivo. Adv Mater **28,** 1809, 2016.
31. Livak, K.J., and Schmittgen, T.D. Analysis of relative gene expression data using real-time quantitative PCR and the 2(−delta delta C(T)) method. Methods **25,** 402, 2001.
32. Hammond, P.T. Building biomedical materials layer-by-layer. Mater Today **15,** 196, 2012.
33. Galiano, R.D., Michaels, J.T., Dobryansky, M., Levine, J.P., and Gurtner, G.C. Quantitative and reproducible murine model of excisional wound healing. Wound Repair Regen **12,** 485, 2004.
34. Huang, M., Chan, D.A., Jia, F., *et al.* Short hairpin RNA interference therapy for ischemic heart disease. Circulation **118,** S226, 2008.
35. Ge, Q., Dallas, A., Ilves, H., Shorenstein, J., Behlke, M.A., and Johnston, B.H. Effects of chemical modification on the potency, serum stability, and immunostimulatory properties of short shRNAs. RNA **16,** 118, 2010.
36. Lennox, K.A., Owczarzy, R., Thomas, D.M., Walder, J.A., and Behlke, M.A. Improved performance of anti-miRNA oligonucleotides using a novel non-nucleotide modifier. Mol Ther Nucleic Acids **2,** e117, 2013.
37. Kioka, N., Ito, T., Yamashita, H., *et al.* Crucial role of vinexin for keratinocyte migration in vitro and epidermal wound healing in vivo. Exp Cell Res **316,** 1728, 2010.
38. Robbins, M., Judge, A., and MacLachlan, I. siRNA and innate immunity. Oligonucleotides **19,** 89, 2009.
39. Judge, A.D., Bola, G., Lee, A.C., and MacLachlan, I. Design of noninflammatory synthetic siRNA mediating potent gene silencing in vivo. Mol Ther **13,** 494, 2006.
40. Marques, J.T., Devosse, T., Wang, D., *et al.* A structural basis for discriminating between self and nonself double-stranded RNAs in mammalian cells. Nat Biotechnol **24,** 559, 2006.
41. Decher, G. Fuzzy nanoassemblies: toward layered polymeric multicomposites. Science **277,** 1232, 1997.
42. Bauer, K., Rock, K., Nazzal, M., Jones, O., and Qu, W. Pressure ulcers in the United States' inpatient population from 2008 to 2012: results of a Retrospective Nationwide Study. Ostomy Wound Manage **62,** 30, 2016.
43. Johnston, B.R., Ha, A.Y., Brea, B., and Liu, P.Y. The mechanism of hyperbaric oxygen therapy in the treatment of chronic wounds and diabetic foot ulcers. R I Med J **99,** 26, 2016.
44. Dinh, T.L., and Veves, A. The efficacy of Apligraf in the treatment of diabetic foot ulcers. Plast Reconstr Surg **117,** 152S, 2006.
45. Glass, G.E., and Nanchahal, J. The methodology of negative pressure wound therapy: separating fact from fiction. J Plast Reconstr Aesthet Surg **65,** 989, 2012.
46. Marston, W.A., Hanft, J., Norwood, P., and Pollak, R.; Dermagraft Diabetic Foot Ulcer Study Group. The efficacy and safety of Dermagraft in improving the healing of chronic diabetic foot ulcers: results of a prospective randomized trial. Diabetes Care **26,** 1701, 2003.
47. Veves, A., Sheehan, P., and Pham, H.T. A randomized, controlled trial of Promogran (a collagen/oxidized regenerated cellulose dressing) vs standard treatment in the management of diabetic foot ulcers. Arch Surg **137,** 822, 2002.
48. Wieman, T.J., Smiell, J.M., and Su, Y. Efficacy and safety of a topical gel formulation of recombinant human platelet-derived growth factor-BB (becaplermin) in patients with chronic neuropathic diabetic ulcers. A phase III randomized placebo-controlled double-blind study. Diabetes Care **21,** 822, 1998.
49. Gould, L., Abadir, P., Brem, H., *et al.* Chronic wound repair and healing in older adults: current status and future research. Wound Repair Regen **23,** 1, 2015.
50. Ceradini, D.J., and Gurtner, G.C. Homing to hypoxia: HIF-1 as a mediator of progenitor cell recruitment to injured tissue. Trends Cardiovasc Med **15,** 57, 2005.
51. Ceradini, D.J., Kulkarni, A.R., Callaghan, M.J., *et al.* Progenitor cell trafficking is regulated by hypoxic gradients through HIF-1 induction of SDF-1. Nat Med **10,** 858, 2004.
52. Ceradini, D.J., Yao, D., Grogan, R.H., *et al.* Decreasing intracellular superoxide corrects defective ischemia-induced new vessel formation in diabetic mice. J Biol Chem **283,** 10930, 2008.
53. Chen, J.S., Longaker, M.T., and Gurtner, G.C. Murine models of human wound healing. Methods Mol Biol **1037,** 265, 2013.
54. Gurtner, G.C., Werner, S., Barrandon, Y., and Longaker, M.T. Wound Repair and Regeneration. Nature **453,** 314, 2008.
55. Maan, Z.N., Januszyk, M., Rennert, R.C., *et al.* Noncontact, low-frequency ultrasound therapy enhances neovascularization and wound healing in diabetic mice. Plast Reconstr Surg **134,** 402e, 2014.
56. Rennert, R.C., Rodrigues, M., Wong, V.W., *et al.* Biological therapies for the treatment of cutaneous wounds: phase III and launched therapies. Expert Opin Biol Ther **13,** 1523, 2013.
57. Rennert, R.C., Sorkin, M., Januszyk, M., *et al.* Diabetes impairs the angiogenic potential of adipose-derived stem cells by selectively depleting cellular subpopulations. Stem Cell Res Ther **5,** 79, 2014.
58. Thangarajah, H., Vial, I.N., Grogan, R.H., *et al.* HIF-1alpha dysfunction in diabetes. Cell Cycle **9,** 75, 2010.
59. Wong, V.W., Gurtner, G.C., and Longaker, M.T. Wound healing: a paradigm for regeneration. Mayo Clin Proc **88,** 1022, 2013.
60. Wong, V.W., Sorkin, M., Glotzbach, J.P., Longaker, M.T., and Gurtner, G.C. Surgical approaches to create murine models of human wound healing. J Biomed Biotechnol **2011,** 969618, 2011.
61. Chang, E.I., Loh, S.A., Ceradini, D.J., *et al.* Age decreases endothelial progenitor cell recruitment through decreases in hypoxia-inducible factor 1alpha stabilization during ischemia. Circulation **116,** 2818, 2007.

62. Duscher, D., Maan, Z.N., Whittam, A.J., *et al.* Fibroblast-specific deletion of hypoxia inducible factor-1 critically impairs murine cutaneous neovascularization and wound healing. Plast Reconstr Surg **136,** 1004, 2015.
63. Egger, M., Schgoer, W., Beer, A.G., *et al.* Hypoxia up-regulates the angiogenic cytokine secretoneurin via an HIF-1alpha- and basic FGF-dependent pathway in muscle cells. FASEB J **21,** 2906, 2007.
64. Hirsch, T., Spielmann, M., Zuhaili, B., *et al.* Human beta-defensin-3 promotes wound healing in infected diabetic wounds. J Gene Med **11,** 220, 2009.
65. Hong, W.X., Hu, M.S., Esquivel, M., *et al.* The role of hypoxia-inducible factor in wound healing. Adv Wound Care (New Rochelle) **3,** 390, 2014.
66. Loh, S.A., Chang, E.I., Galvez, M.G., *et al.* SDF-1 alpha expression during wound healing in the aged is HIF dependent. Plast Reconstr Surg **123,** 65S, 2009.
67. Velander, P., Theopold, C., Bleiziffer, O., *et al.* Cell suspensions of autologous keratinocytes or autologous fibroblasts accelerate the healing of full thickness skin wounds in a diabetic porcine wound healing model. J Surg Res **157,** 14, 2009.
68. Zimmermann, A.S., Morrison, S.D., Hu, M.S., *et al.* Epidermal or dermal specific knockout of PHD-2 enhances wound healing and minimizes ischemic injury. PLoS One **9,** e93373, 2014.
69. Huang, X., Le, Q.T., and Giaccia, A.J. MiR-210–micromanager of the hypoxia pathway. Trends Mol Med **16,** 230, 2010.
70. Jang, Y.C., Arumugam, S., Gibran, N.S., and Isik, F.F. Role of alpha(v) integrins and angiogenesis during wound repair. Wound Repair Regen **7,** 375, 1999.

Address correspondence to:
Brian H. Johnston, PhD
2161 Delaware Avenue, Ste. E
SomaGenics, Inc.
Santa Cruz, CA 95060

E-mail: bjohnston@somagenics.com

or

Geoffrey C. Gurtner, MD, FACS
Stanford University School of Medicine
Department of Surgery
Division of Plastic
and Reconstructive Surgery
257 Campus Drive West
Hagey Building GK-201
Stanford, CA, 94305-5148

E-mail: ggurtner@stanford.edu

Received: November 22, 2017
Accepted: March 1, 2018
Online Publication Date: June 27, 2018